

## Supporting Information

### **Large scale and cost effective generation of 3D self-supporting oxide nanowire architectures by a top-down and bottom-up combined approach**

Peixun Fan,<sup>\*ab</sup> Minlin Zhong,<sup>\*a</sup> Benfeng Bai,<sup>b</sup> Guofan Jin<sup>b</sup> and Hongjun Zhang<sup>a</sup>

<sup>a</sup>*Laser Materials Processing Research Centre, School of Materials Science and Engineering, Tsinghua University, Beijing 100084, PR China. Emails: fpx@tsinghua.edu.cn, zhml@tsinghua.edu.cn*

<sup>b</sup>*State Key Laboratory of Precision Measurement Technology and Instruments, Department of Precision Instrument, Tsinghua University, Beijing 100084, PR China*

**Table S1.** Laser processing parameters for different substrates

Substrate	Patterns in Figures	Pulse Energy ( $\mu\text{J}$ )	Speed ( $\text{mm s}^{-1}$ )	Spacing ( $\mu\text{m}$ )	Repeat
Cu	Fig. 1b	75	500	50	30
	Fig. 2a	25	500	50	30
	Fig. 2c	75	50	50	1
	Fig. 4	75	50	30	1
	Fig. 5a, c, e	25	500	30, 40, 50	30
	Fig. 6a	175	500	50	30
	Fig. 6d	175	50	30	1
	Fig. 6g	75	500	50	30
Ti6Al4V	Fig. 7	30	500	30	20

Note: the wavelength, pulse duration, and pulse repetition rate are kept constant for all cases above to be 1030 nm, 800 fs, and 200k Hz, respectively.

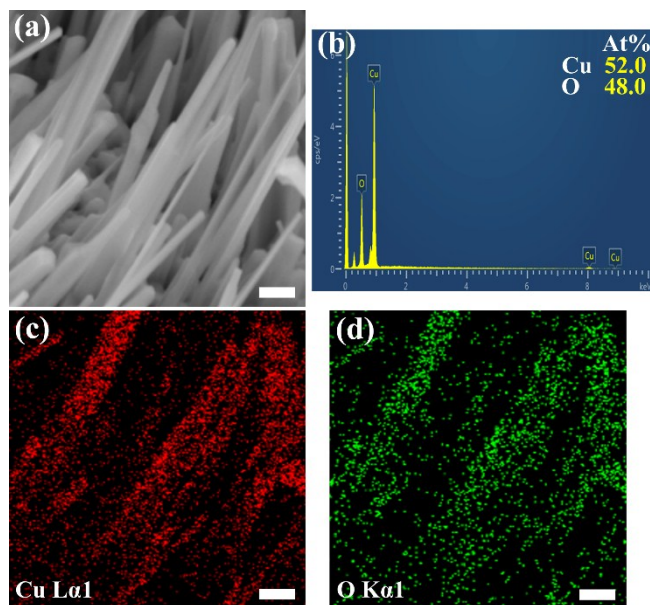


**Fig. S1.** Composition detection of the nanowires grown on Cu substrate. (a) High magnification SEM image for the nanowires. (b) EDS spectrum of Cu and O elements recorded in (a). (c) and (d) Elemental mapping of Cu  $L\alpha 1$  and O  $K\alpha 1$  contained in the nanowires. All scale bars equal 500 nm. (The non-indexed peak in the EDS spectrum represents C element which can come from the organic compounds absorbed by the oxide surfaces from the surrounding atmosphere.)

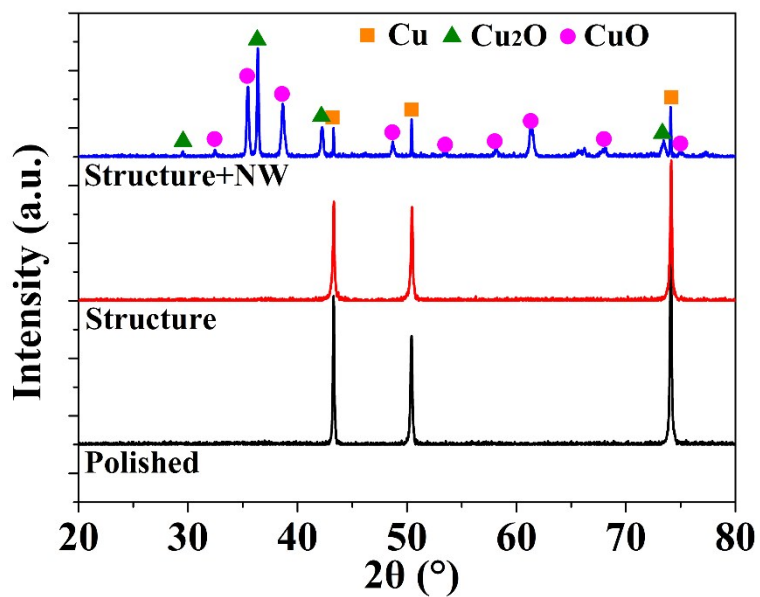


**Fig. S2.** XRD patterns of Cu surfaces in different conditions. As can be seen, most diffraction peaks newly appeared after growing nanowires represent  $\text{CuO}$  phase. Those representing  $\text{Cu}_2\text{O}$  result from the insufficiently oxidized subsurface layers.

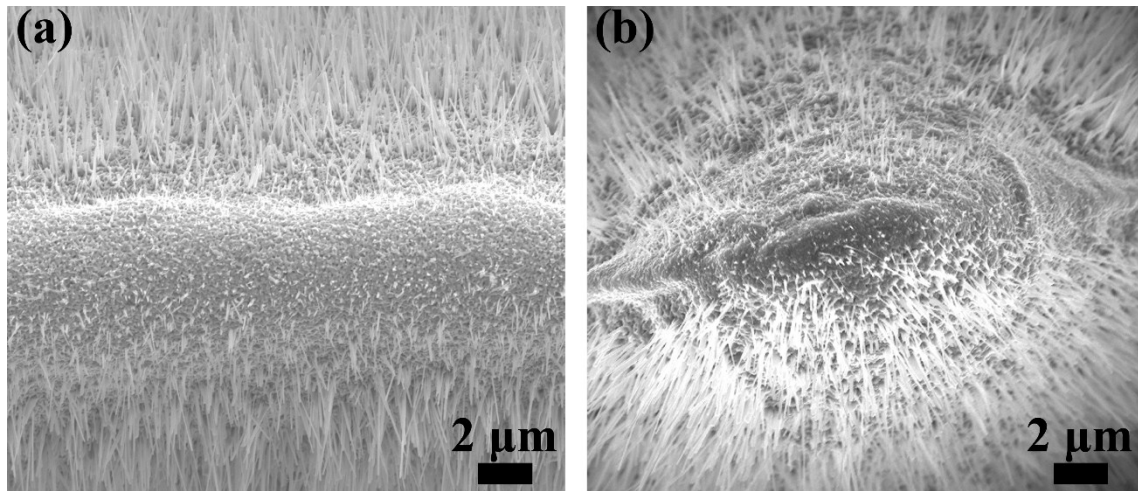


**Fig. S3.** Highly magnified SEM images of nanowires grown on laser fabricated (a) 1D and (b) 2D periodic structures.

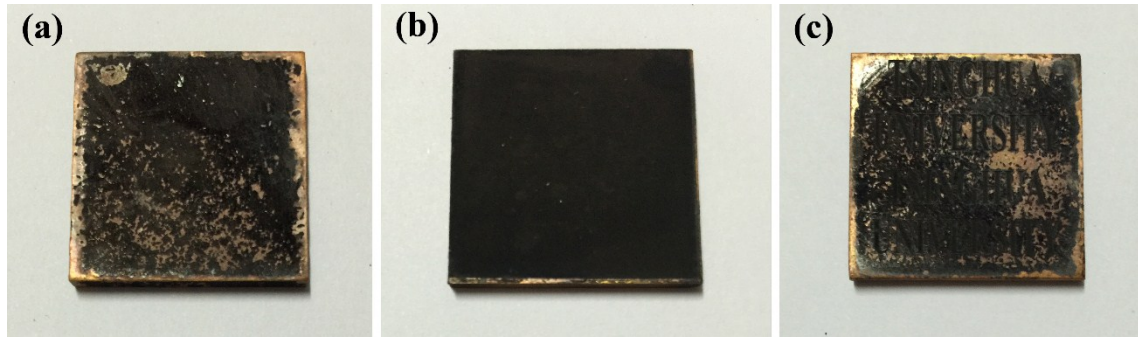


**Fig. S4.** Photographs of (a) polished Cu surface, (b) Cu surface completely treated by ultrafast laser, and (c) Cu surface treated by ultrafast laser in the pattern of “TSINGHUA UNIVERSITY” after thermal oxidation treatment. Dimensions for all the three samples are  $25\times 25\times 3\text{ mm}^3$ .

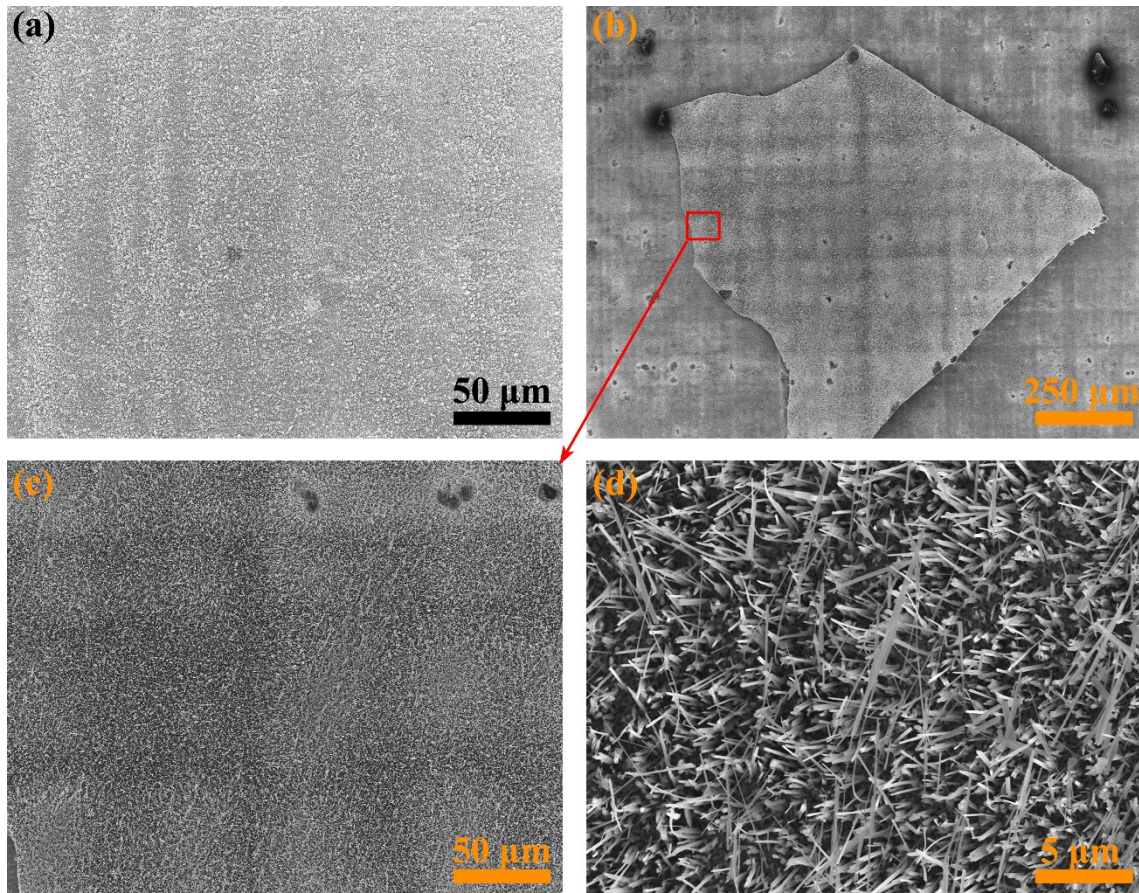


**Fig. S5.** SEM images for Cu surface with only ultrafast laser fabricated sub-microscale structures:  
(a) Before thermal oxidation; (b) (c) (d) After thermal oxidation.

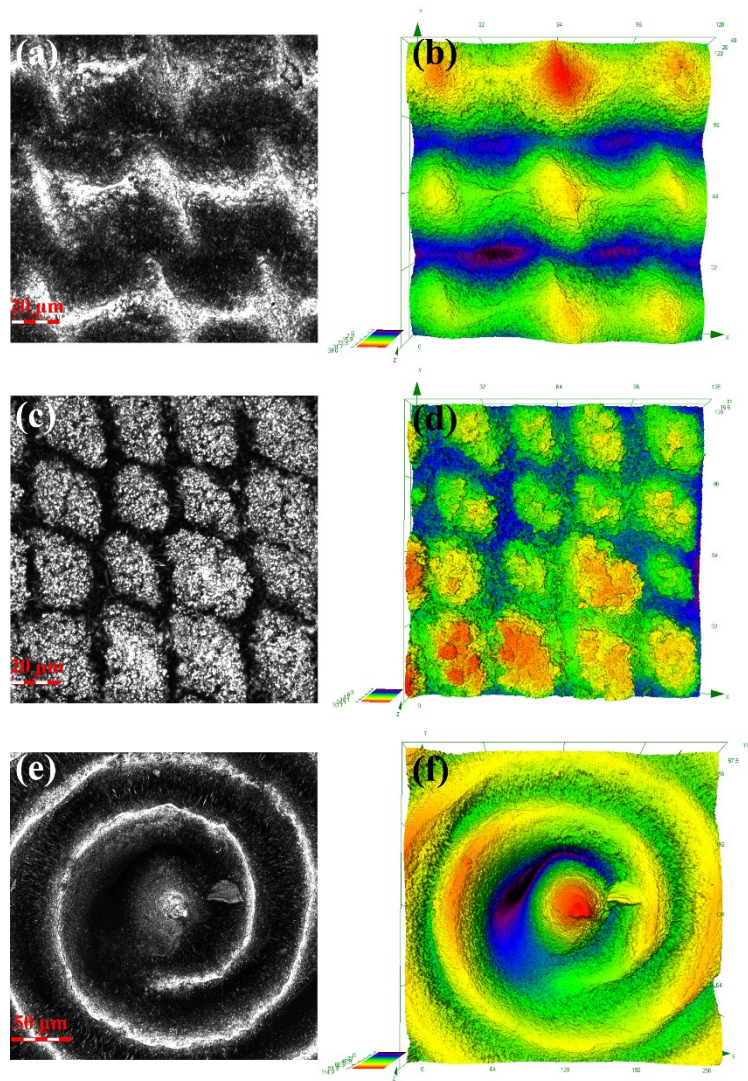


**Fig. S6.** 3D laser confocal microscope images for the ultrafast laser fabricated (a) (b) 2D disordered structures, (c) (d) particle cluster structures, (e) (f) helical structures with nanowires in grey (a) (c) (e) and color (b) (d) (f) charts.



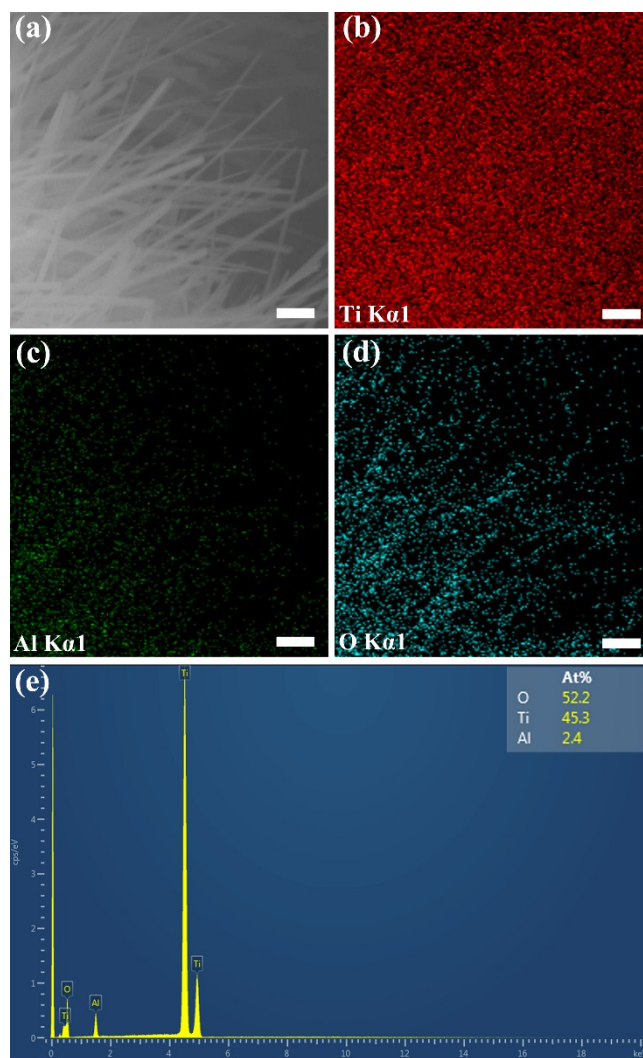


**Fig. S7.** Composition detection of the nanowires grown on Ti6Al4V substrate. (a) High magnification SEM image for the nanowires. (b), (c) and (d) Elemental mapping of Ti K $\alpha$  1, Al K $\alpha$  1 and O K $\alpha$  1 contained in the nanowires. (e) EDS spectrum of Ti, Al and O elements recorded in (a). All scale bars equal 500 nm.

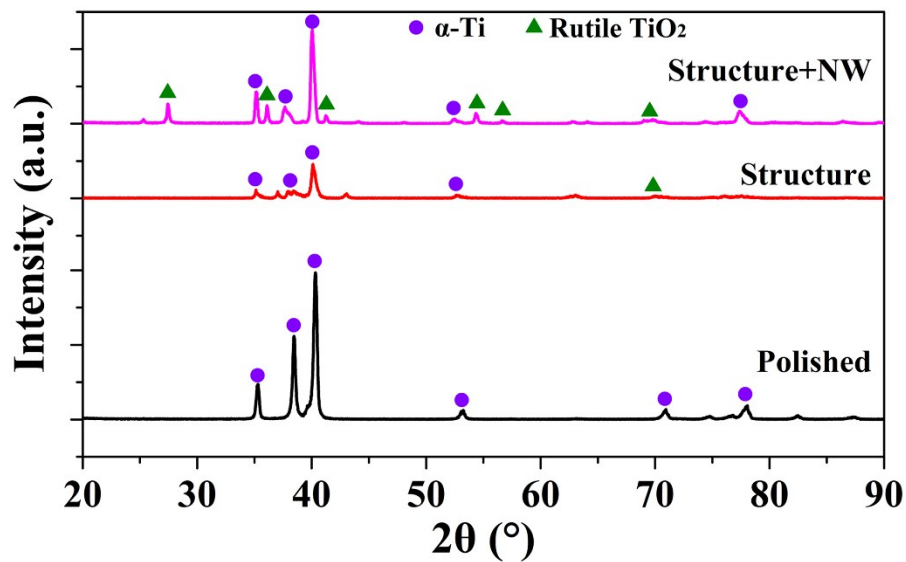


**Fig. S8.** XRD patterns of Ti6Al4V surfaces in different conditions. As can be seen, the diffraction peaks representing  $\text{TiO}_2$  phase appeared apparently after growing nanowires on the laser structured Ti6Al4V surfaces.